EUROFUSION WPMAT-PR(15) 13612

E. Tejado et al.

The effects of tantalum addition on the microtexture and mechanical behaviour of tungsten for ITER applications

Preprint of Paper to be submitted for publication in
Journal of Nuclear Materials

This work has been carried out within the framework of the EUROfusion Consortium and has received funding from the Euratom research and training programme 2014-2018 under grant agreement No 633053. The views and opinions expressed herein do not necessarily reflect those of the European Commission.

The effects of tantalum addition on the microtexture and mechanical behaviour of tungsten for ITER applications

E. Tejado[1,2], A. Munoz[3], P.A. Carvalho[4,5], M. Dias[4], J.B. Correia[4,6], U.V. Mardolcar[4,7], J.Y. Pastor[1]*

[1] *Departamento de Ciencia de Materiales-CIME, ETSI Caminos, Canales y Puertos, Universidad Politécnica de Madrid, Madrid, Spain.*
[2] *Centro Nacional de Investigaciones Metalúrgicas (CSIC), Madrid, Spain.*
[3] *Departamento de Física, Universidad Carlos III, Leganés, Spain.*
[4] *Associação Euratom/IST, Instituto de Plasmas e Fusão Nuclear, Instituto Superior Técnico, Universidade Técnica de Lisboa, Av. Rovisco Pais, 1049-001 Lisboa, Portugal.*
[5] *ICEMS, Departamento de Bioengenharia, Instituto Superior Técnico, Av. Rovisco Pais, 1049-001 Lisboa, Portugal.*
[6] *LNEG, Laboratório Nacional de Energia e Geologia, Estrada do Paço do Lumiar, 1649-038 Lisboa, Portugal.*
[7] Centro de Química Estrutural, Instituto Superior Técnico, Universidade de Lisboa,
Av. Rovisco Pais,1049-001 Lisboa, Portugal.
elena.tejado@mater.upm.es

ABSTRACT

W and its alloys are very promising materials for producing plasma facing components (PFCs) in the near future fusion power reactors, even as a structural part in it. However, whereas the properties of tungsten are suitable for a PFC, its structural applications are still narrowed for its low toughness, ductile to brittle transition temperature and recrystallization behaviour. Therefore, many efforts have been made to improve its performance by alloying tungsten with other elements.

Hence, in this investigation, the thermo-mechanical performance of two new tungsten-tantalum materials has been evaluated. Materials with W-5wt.%Ta and W-15wt.%Ta were processed by mechanical alloying (MA) and later consolidation by hot isostatic pressing (HIP), with distinct settings for each composition. Thus, it was possible to determine the relationship between the microstructure and the addition of Ta with the macroscopic mechanical properties. They were measured by means of hardness, flexural strength and fracture toughness, those last ones, in the temperature range of 300 to 1473 K. The microstructure and the fracture surfaces features of the tested materials were analysed by Field Emission Scanning Electron Microscopy (FESEM).

Keywords: tungsten, tantalum, mechanical properties, high temperature, nuclear applications.

1. Introduction

Fusion is the least developed of the alternatives to non-renewable energy resources, but it has nevertheless a high potential for future energy supply since its raw materials are largely available. However, one of the main obstacles faced for the development of a fusion plant is the designing of materials that will tolerate the harsh radiation environment combined with a strong mechanical stress [1]. Tungsten and tungsten alloys are some of the candidate armor materials for the plasma facing components of the International Thermonuclear Experimental Reactor and its previous

prototype DEMO. For the present reference design tungsten has been selected as armor for the divertor, the upper vertical target, dome, cassette liner, and for lower baffle because of its unique resistance to ion and charge-exchange particle erosion in comparison with other materials [2].

For those applications, different tungsten grades (pure, dispersion strengthened and cast alloys) have been considered. However, the mechanical properties of commercially available tungsten are not yet adequate for structural purposes due to the intrinsic brittleness of tungsten at low temperatures, as the ductile-brittle transitions (DBTT) occur in the vicinity of 0.15 T_m, thus limiting the operating temperatures of the reactor. On the other hand, W mechanical properties at high temperature are quite poor, and it exhibits a strong degradation in air due to its linear oxidation.

The approaches towards reducing brittleness of W at low temperatures have not changed since 1975, as reported by W.D. Kropp [3], those are: i) the improvement of purity, ii) maintenance of a fine-grained or worked structure, iii) incorporation of inert dispersoids, and iv) alloying to promote solution softening. It has been found that addition of certain elements, such as Re, Tc, Ti or Co [4] can improve the ductility of W thus reducing the DBTT of the alloy. However, some of these elements become activated under neutron irradiation, such as, Co or Re, this last one, even forms brittle sigma-phases precipitates with the primary products of its nuclear reactions (W-Re-Os) [5].

After rejecting the W–Re alloys for economic and practical reasons, it has been put forward that sintered W heavy alloys (WHA) might fulfill the requirements of the current divertor designs. In particular, the addition of other refractory metals could lead to an improved tungsten product for divertor applications, as the high melting point, high thermal conductivity and high resistance to sputtering and erosion are shared. Among this approach, Ta could be one of the most auspicious alloying elements [6], since it forms solid solution with W, does not produce new phases after transmutation and has been widely used to alloy low activation ferritic-martensitic steels in order to reduce their DBTT [7] [8].

Quite few researches have been carried out on the tungsten-rich end of the binary W-Ta system. Therefore this paper is focused on the influence of both microstructure and chemical composition on the fracture behavior of two tungsten-tantalum alloys as function of temperature. The diverse initial particles sizes and different milling times during manufacturing led to two materials approaches: W-5 wt. %Ta alloy and W-15 wt. %Ta composite. To characterize this, three point bending and fracture toughness tests were performed in the temperature interval from 25 °C to 1200 °C. Additional studies were carried out in order to determine the thermal diffusivity of one of the sintered products as well as a basic physical characterization.

2. Experimental details

2.1. Materials and sample preparation

Two tungsten materials containing 5 wt. %Ta (5.12 at. %) and approximately 15 wt. %Ta (14.8 wt. % and 15 at. %), have been studied. They were both obtained by Hot Isostatic Pressure (HIP) of blended and ball milled powders. In an effort to better evaluate the influence of the processing parameters on the mechanical performance; those were modified for each material.

Firstly, W-5 wt. %Ta was prepared mixing together elemental powders of pure W (99.9%, median particle size 1-5 µm) and Ta (99.9 %, median particle size less than 2µm) in a tubular T2F mixer for 4 h. Afterwards, blended powders were milled for 50 h in a high-energy planetary mill under a high purity Ar atmosphere, WC container and WC balls of Ø 10 mm with a 4:3 ball-to-powder ratio, as

grinding media, were used. Before the consolidation, the alloyed powders were encapsulated in a steel container and degassed for 24 h at 400 °C in a vacuum of $\sim 2 \times 10^{-3}$ mbar.

Alternatively, for W-15 wt. % Ta, W powder (99.95 %, median particle size 1 µm) was mixed with Ta powder (99.95 %, median particle size 75 µm) in a Retsch PM400MA planetary ball mill for 4 hours under high purity Ar atmosphere mill to obtain W-15 wt. % Ta composite. Further details of the production and microstructural characterization of W-15 wt. % Ta can be found in [9].

Afterwards, both materials were deoxidized in an Ar + 10 % H_2 atmosphere during 3h at 1100 ºC, subsequently canned inside stainless steel cans and degassed at 450 ºC for 24 h in Ar. The encapsulated compacts were then consolidated by hot isostatic pressing for 2 hours at temperatures between 1250 and 1300 °C with high purity Ar under 194 MPa (27 800 psi).

Cylindrical billets of 30 mm in diameter and 50 mm in length were obtained after consolidation by HIP. Miniaturized bend specimens (nominal dimensions 1.7 × 1.7 × 25 mm^3) and small discs with a diameter of 15.7 mm and a height of 2 mm were produced by refrigerated electro-discharge machining to comply the needs of mechanical and thermal-diffusivity testing, respectively.

In addition, pure tungsten was produced as a reference material [10] to serve as basis for comparison with present materials.

2.2. Mechanical Testing

Materials characterization was performed in an extended high temperature range by means of quasi-static three point bending (TPB) tests, on smooth and notched specimens. Additionally it was determined thermal diffusivity in the expected operation temperatures. Hardness (Vickers and Berkovich indentation), elastic modulus and density by the Archimedes method were measured at 300 K.

Vickers micro-hardness was determined applying a load of 9.8 N for 15 s (HV1) in an AKASHI MVK-EIII tester. Additionally, nanoindentation to a depth of 1500 nm was performed on the same samples using a standard Berkovich tip, calibrated using fused silica. Average values of hardness and elastic modulus were taken from the unloading curve according to Oliver and Pharr method [11]. Elastic modulus results where then compared with those obtained by the flexural vibration resonance method (Grindosonic MK4i, J.W. Lemmens, Belgium).

In this investigation, TPB tests were performed with 16 mm span at a constant cross-head travel speed of 100 µm/min, so as to control easily the test process and obtain the accurate recording data. In order to investigate the transition from the ductile to brittle fracture, TPB testing was performed at temperatures between RT and 1000 °C in air with a small silicon carbide furnace mounted inside the loading zone of the INSTRON 3369 testing machine used. However, due to material oxidation at temperatures greater than 600 °C, testing was also carried out in a vacuum environment with a INSTRON 8501 equipped with a high temperature vacuum furnace (Sigmatest GmbH), which allows experiments up to 1600 °C and 10^{-6} mBar vacuum pressure. Flexural strength was computed by Euler-Bernoulli equations for slender beams up to failure, however when yield stress was exceeded, 0.2% strength offsets was reported.

Fracture toughness was also determined by means of TPB configuration in the same environments and temperature range. For this purpose, laser machined notches were introduced in the samples, obtaining with this method a real crack type as seen in Figure 1. Overall notch lengths were measured under scanning electron microscope, yielding mean tip radius of 5-20 nm and crack

lengths of approximately 250 µm. Finally, fracture toughness was computed from the failure load and the beam section using the stress intensity factor for mode I stress supplied by Guinea *et al*. [12].

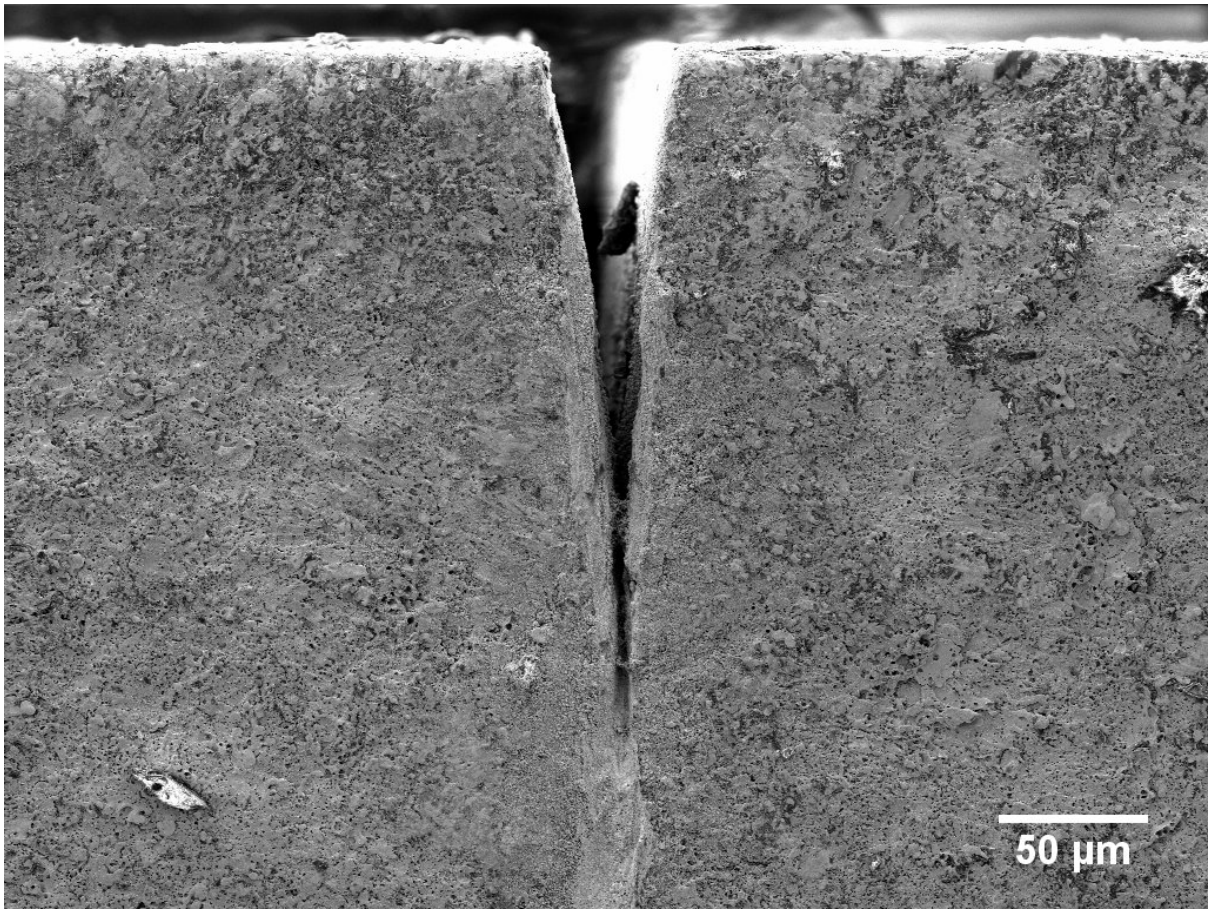

Fig. 1. Scanning electron micrograph of a W-5wt. %Ta fracture toughness sample with laser notch.

Post mortem examinations were performed by scanning electron microscopy (SEM).The analysis of the fracture surfaces of samples tested in air was, however, hindered in the samples tested at 600 °C and above by the presence of an oxide layer. Additionally, RT samples were mounted and polished to study the microstructure and elements distribution by means of energy dispersive X-ray microanalysis.

Thermal diffusivity was measured using the laser flash technique with a FlashLine 5000 Anter Corporation instrument. Measurements were done in vacuum in a temperature range from 300 to 773 K. The technique involves the deposition of heat via a laser pulse on one face of a thin disk specimen and the register of the temperature rise on the other face. Thermal diffusivity is then derived from the time dependence of the measured temperature rise. The apparatus consists of a pulsed laser energy source, a vacuum oven for heating the test specimens, and a data acquisition system [13].

3. Results and discussion

3.1. Microstructure

The study of W-5 wt. % Ta microstructure via metallography and etching with Murakami reagent shows three different phases: i) lagoons of tantalum, ii) large tungsten grains, and iii) Ta(W) solid solution surrounding the W grains (Figure 2).

Due to the long milling time during manufacturing, around 50 h, nanometric grains were produced and are difficult to appreciate, though fracture surfaces (see Figure 3) revealed an average grain size of 50 nm for this Ta(W) phase with coarser grains of W and Ta over several microns. These heterogeneities may stem from the inner core of the powder particles after MA, revealing that although a very effective partial reduction in particle size was observed, the system had not achieved yet steady-state.

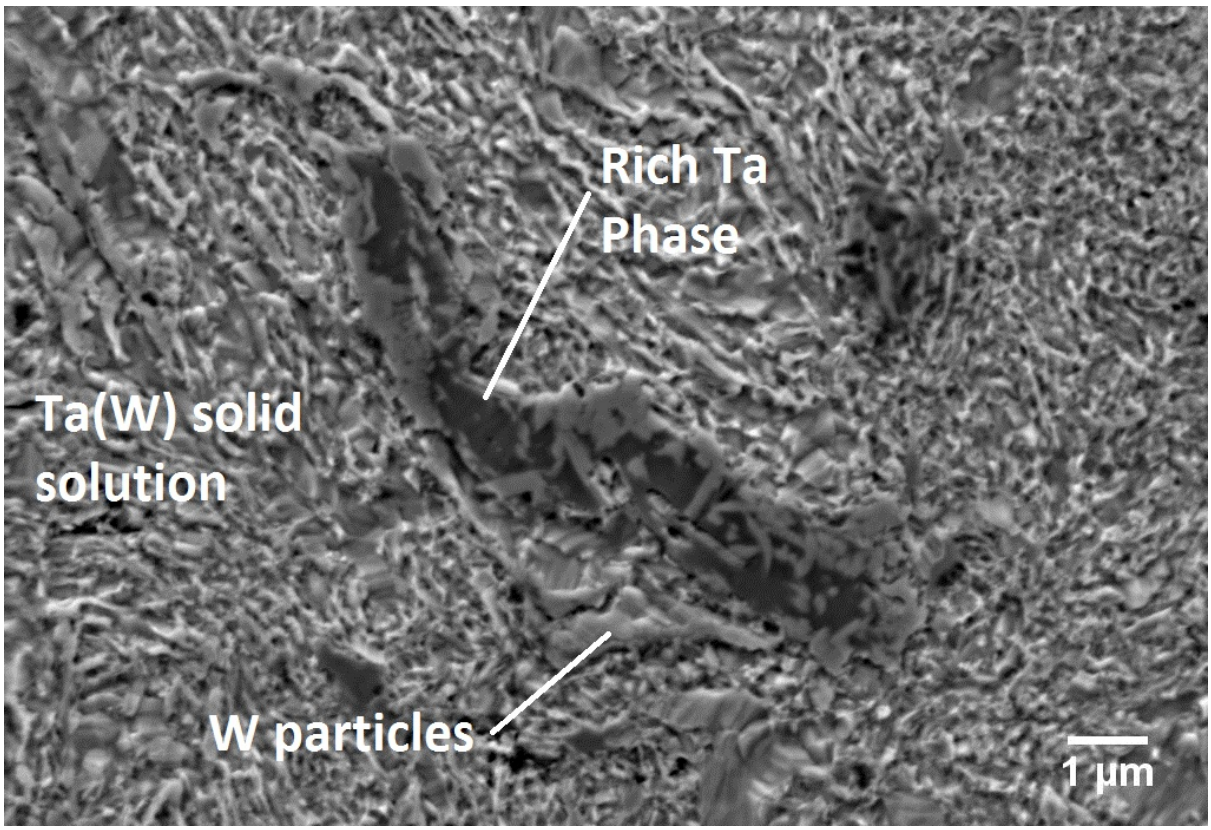

Fig. 2. Scanning electron micrograph of a W-5wt. %Ta sample after etching with Murakami reagent. EDX analysis revealed that dark grey particles correspond to Ta pools, observing the diffusion of W from the Ta(W) solid solution.

Additionally, Figure 3 of a post mortem specimens illustrates that W particles of similar size tend to bring into line in a precise way.

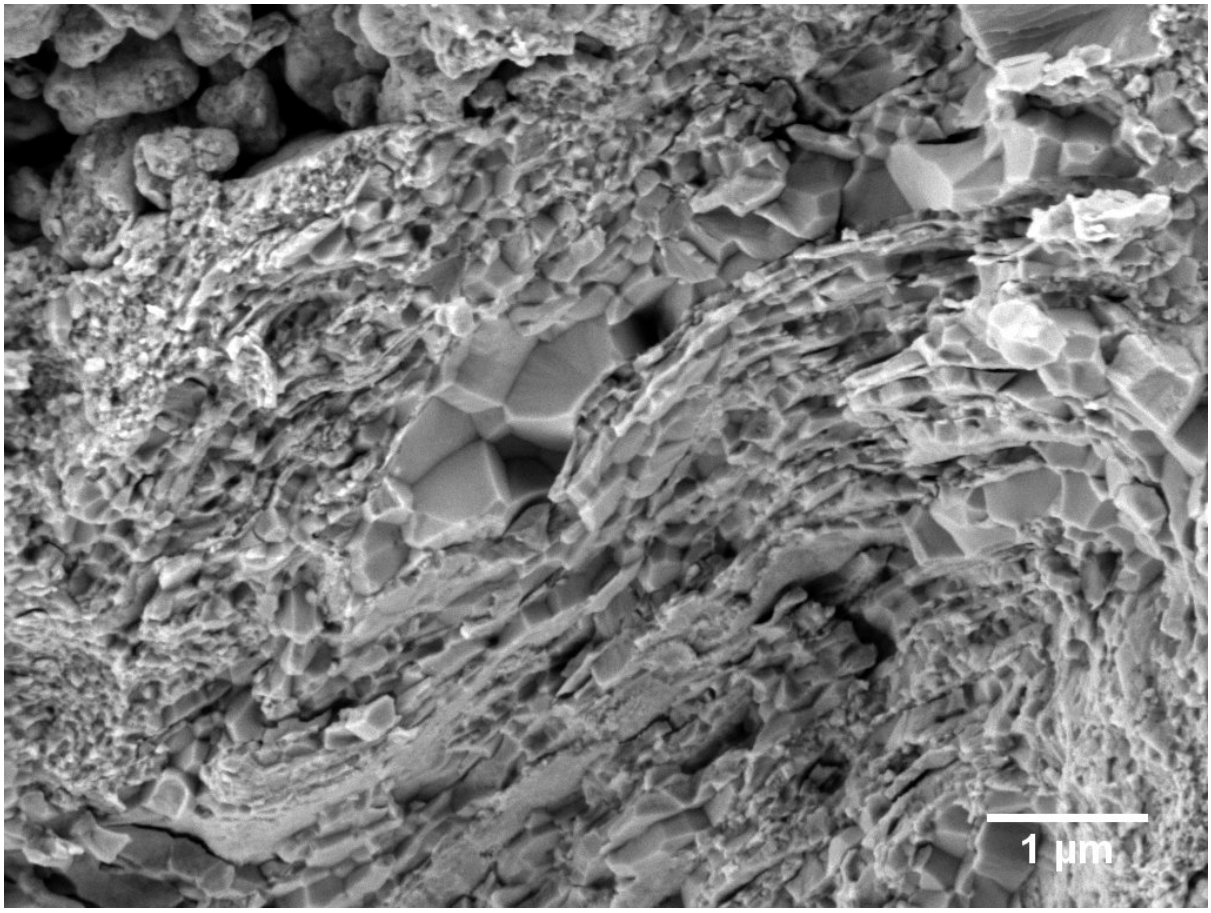

Fig. 3. Fractograph of W-5 wt. % Ta specimen tested at room temperature.

In contrast to the observed for W-5 wt. % Ta, EDX-SEM micrographs of W-15 wt. %Ta composite exemplify a totally different microstructure; it is composed of two clearly phases: a rich W phase and a rich Ta phase, both composed of smaller grains. Nevertheless, as observed from the fractographical analysis, all single grains have sizes smaller than 30 µm, whilst nanometric ones are stick together into larger conglomerates (see Figure 5).

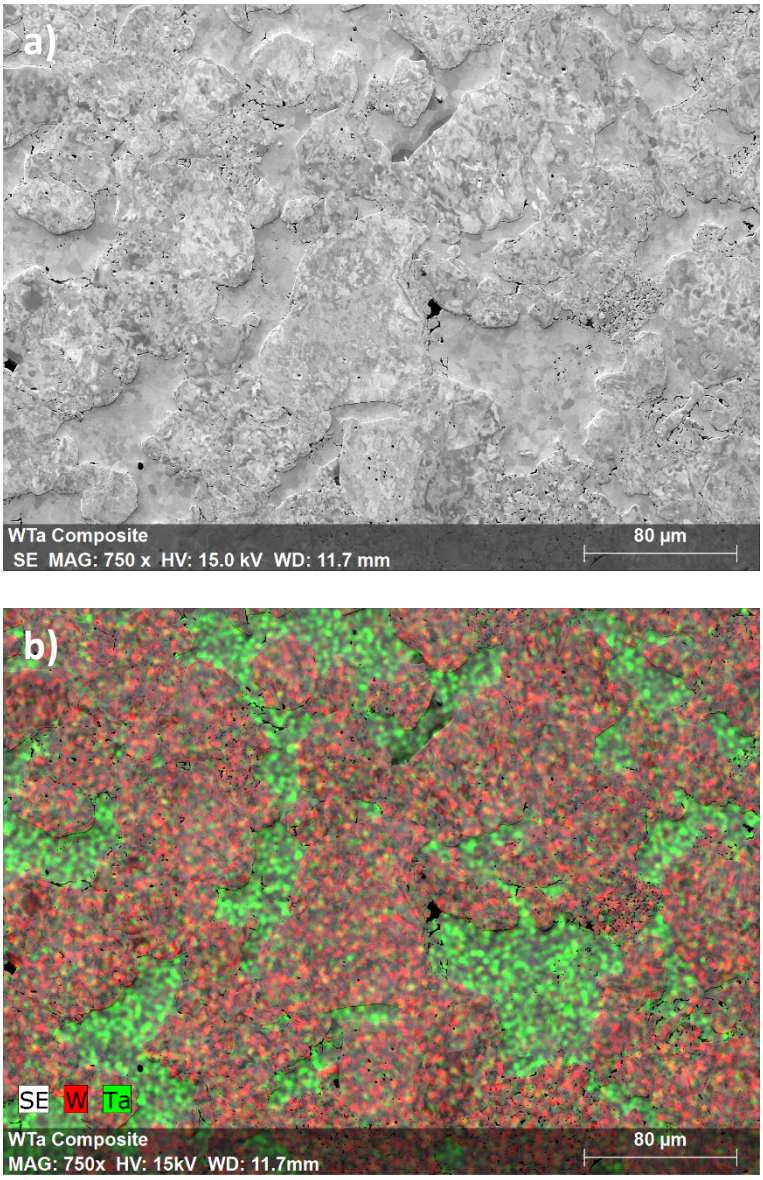

Fig. 4. Scanning electron micrograph of a polished section of the W-15 wt. % Ta composite showing size and distribution of W and Ta phases. (a) Secondary electrons image. (b) EDX-Mapping of W (red) and Ta (green) in (a). The dark spots correspond to porosity (For interpretation of the references to colour in this figure legend, the reader is referred to the web version of this article).

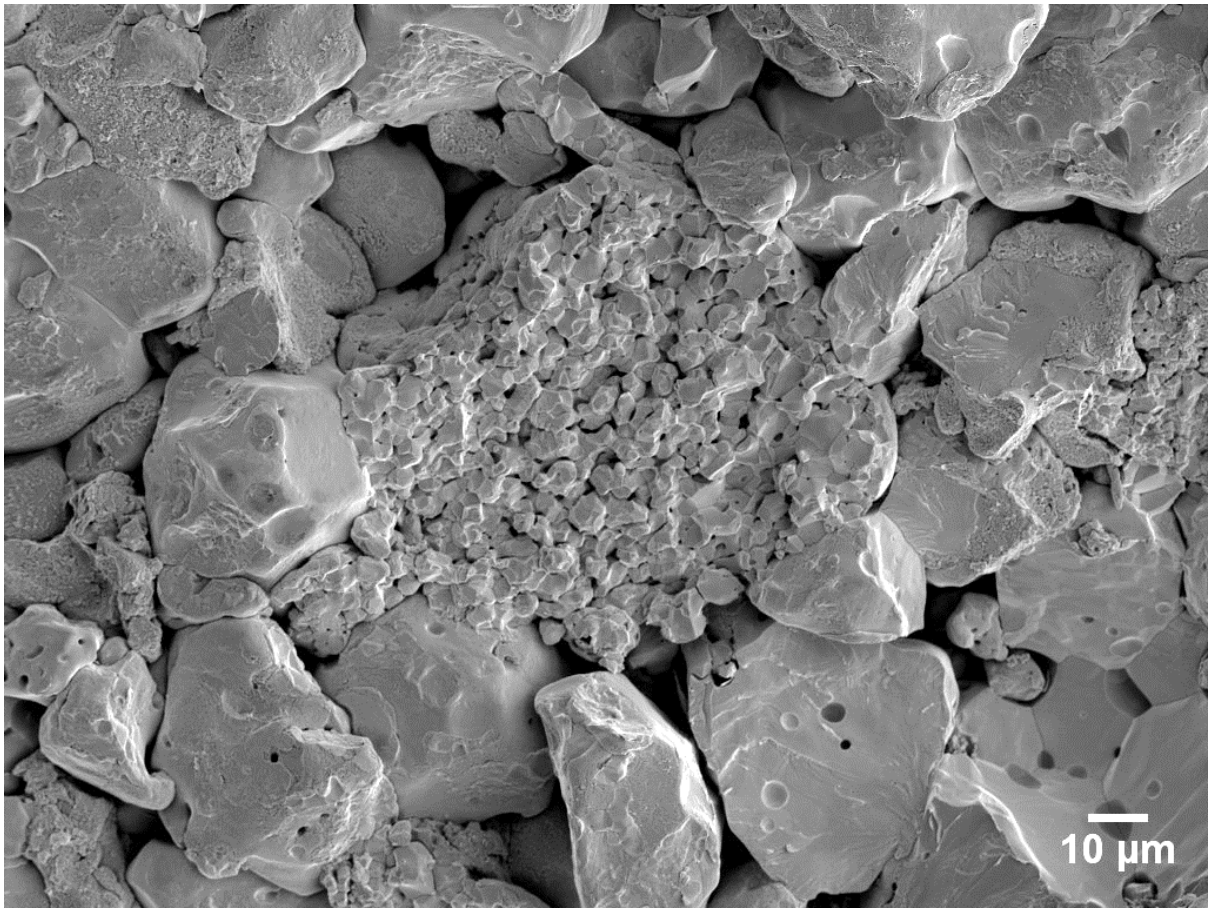

Fig. 5. Fractograph of W-15 wt. % Ta specimen tested at room temperature.

3.2. Mechanical properties

Table 1 shows the materials densities: experimental, theoretical and relative, as well as the calculated porosity. Densification was determined to lie between 91.81 of the theoretical value for W–5 wt. %Ta and 92.96 % for W–15 wt. %Ta, whilst the relative density of our reference pure tungsten was 91.64%. This indicates an increase in the densification with the content of Ta, even after an extended milling time for W-5 wt. % Ta material. In consequence, no clear correlation of the densification after HIP with the manufacturing conditions can be deduced from these results. Nevertheless, porosity could be attributed to the Kirkendall effect, as the maximum temperature reached during the HIP process, 1300 °C, represents only 0.43 T_{hom} for tantalum and just 0.39 T_{hom} for tungsten.

Table 1. Density of pure tungsten, W–5 wt. % Ta and W-15 wt. % Ta materials

Alloy	Experimental (g/cm^3)	Theoretical (g/cm^3)	Relative (%)	Porosity (%)
Pure W [11]	17.64±0.02	19.25	91.64	8.36
W-5 wt. % Ta	17.54±0.01	19.10	91.81	8.19
W-15 wt. % Ta	17.49±0.12	18.82	92.96	7.04

At the same time, the measured hardness, HV and nH, significantly increases from pure tungsten to W-Ta materials, being three times higher in the case of W-5 wt. % Ta. Whereas, W-15 wt. % Ta exhibits approximately twice the hardness of pure W (Fig. 6). This indicates an increase in mechanical strength but also brittleness with Ta content, as will be confirmed later on.

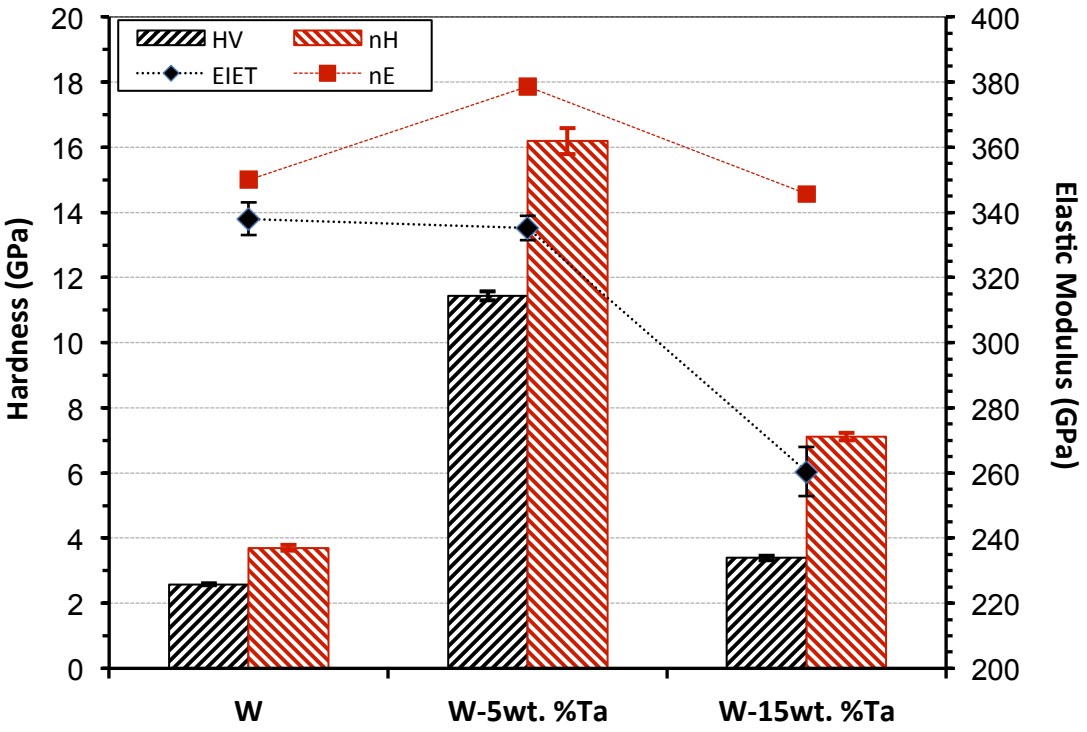

Fig. 6. Vickers hardness (HV), Berkovich instrumented nano-indentation hardness (nH), elastic modulus measured with the impulse excitation technique (EIET) and elastic modulus from nano-indentation tests (nE) for pure W, W-5wt. %Ta and W-15wt. % Ta.

Furthermore, results obtained after nanoindentation tests can be correlated with microstructure according to the Hall-Petch equation [14], which establishes that the decrease of grain size improves the mechanical properties, i.e. hardness and yield stress (see Fig. 9). Therefore, this correlation can also be established for microhardness tests, whose values are slightly lower than the ones obtained by nanoindentation. This variance is attributed to the different definition of hardness for both tests, projected contact area versus indenter contact area. Figure 7 shows the indentation matrix performed in W-15 wt. % Ta, where both phases where tested. On the other hand, when analysing elastic modulus, it was not easy to identify clear tendencies due to the important influence of porosity on elastic modulus but also of phases and grains sizes. Nevertheless, the values exhibit the order of magnitude expected for tungsten alloys.

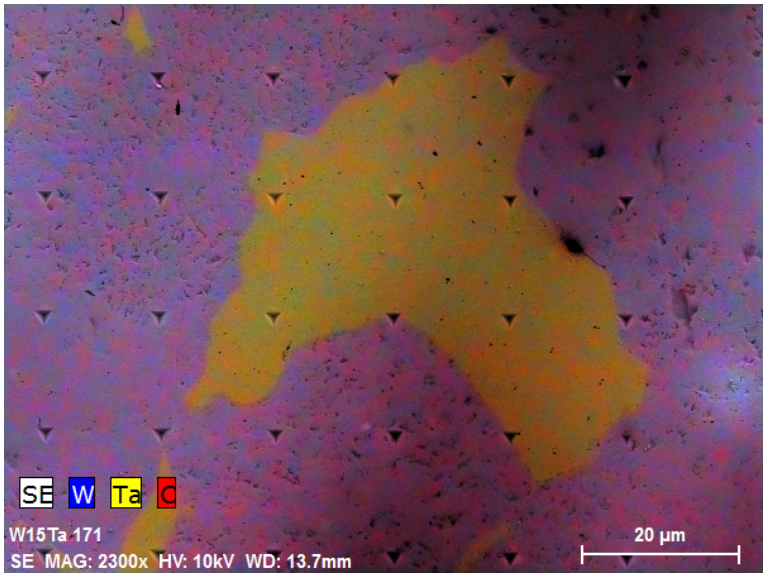

Fig. 7. Scanning electron micrograph of W-15 wt. % Ta with EDX-Mapping of W (blue) and Ta (yellow) phases and Berkovich indentation matrix. (For interpretation of the references to colour in this figure legend, the reader is referred to the web version of this article.)

- ***Flexural strength***

The TPB testing produced load-displacement data spanning a temperature range of 298-1273 K (25-1000 °C) in air and 673-1473K (400-1200 °C) in inert/vacuum atmosphere. These data have been converted to stress-strain and presented in Figure 7.

The tests results show that the W-5 wt. % Ta alloy exhibits a significantly higher strength as well as a higher DBTT – around 1373 K – than the W-15 wt. % Ta material. W-5 wt. % Ta specimens failed by brittle fracture at low temperatures and a transition from brittle to ductile fracture behaviour can be observed with increasing temperature marked by a steep increase of flexural strength at 1373 K, up to this temperature, the degradation of the material is evident. Whilst W-5 wt. % Ta material appears to have a very abrupt DBTT in the range 1273-1373 K, W-15 wt. % Ta exhibits an smooth transition from brittle to ductile fracture, starting at about 673 K but being fully visible over 1073 K.

FEG-SEM examination of the fracture surfaces reveals that W-5 wt. % Ta shows an intergranular brittle fracture below 1273 K. Above, the first local traces of ductile fracture appeared, in agreement with the observed plastic behaviour in Fig. 7.a. Besides, at higher temperatures the properties had completely degraded even under a vacuum atmosphere, most likely due to the porosity decreasing the alloy cohesion.

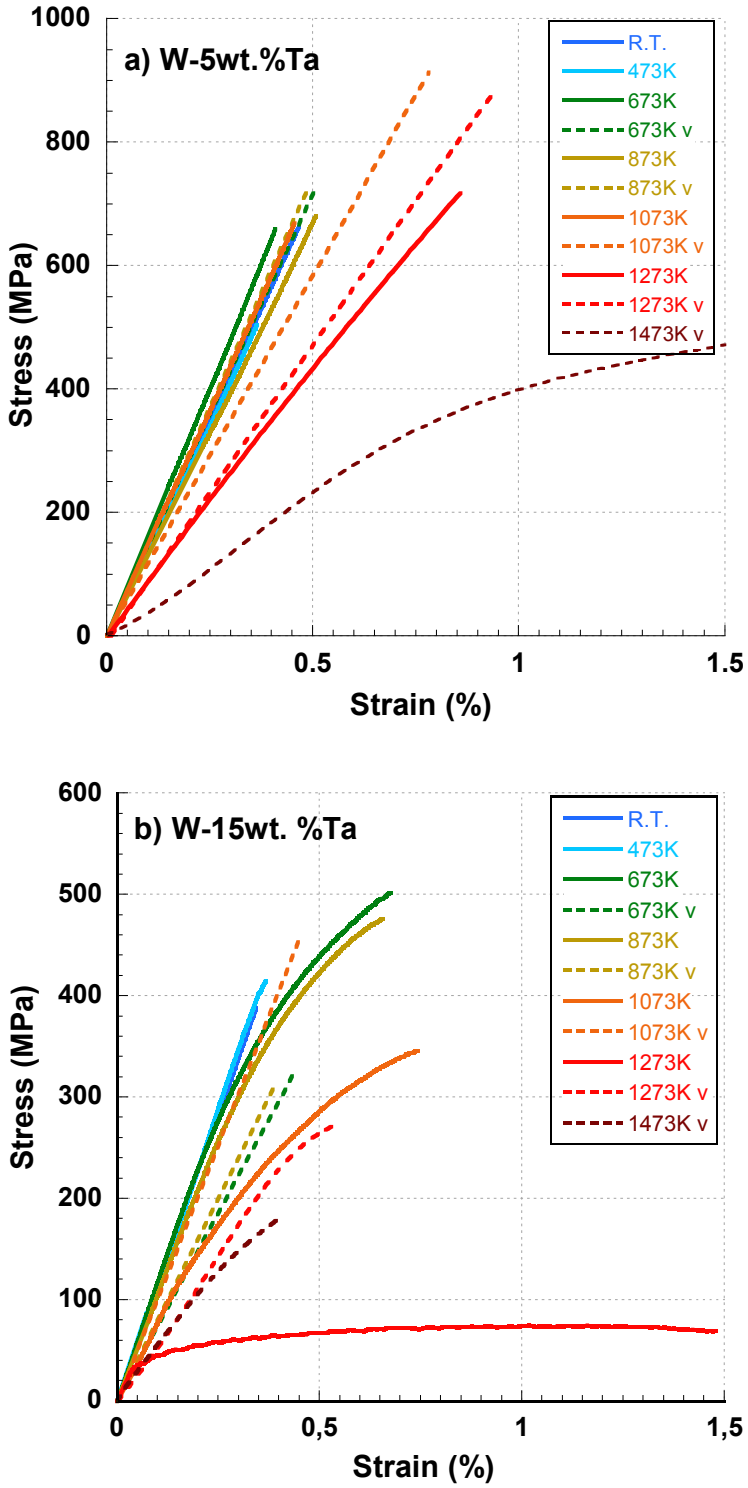

Fig. 8. Stress–strain curves from non-standard three-point bending tests on: a) W-5wt. %Ta and b) W-15wt. %Ta at different temperatures. Dashed lines represent tests performed in vacuum atmosphere. (For interpretation of the references to colour in this figure legend, the reader is referred to the web version of this article.)

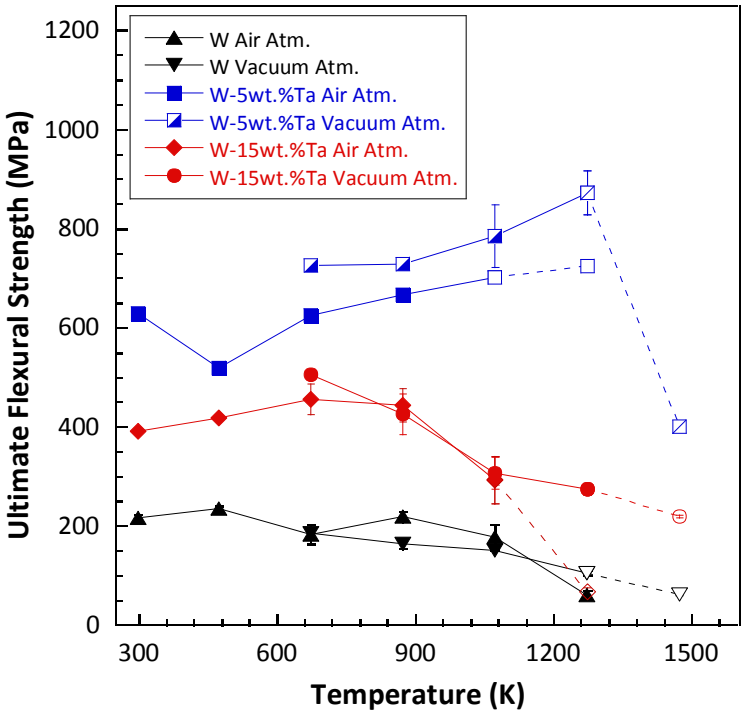

Fig. 9. Ultimate flexural strength versus test temperature for W-5wt. %Ta, W-15wt. %Ta and pure tungsten in air and vacuum atmospheres. The open symbols and dashed lines represent the yield strength at 0.2 % when the materials exhibited a ductile behaviour.

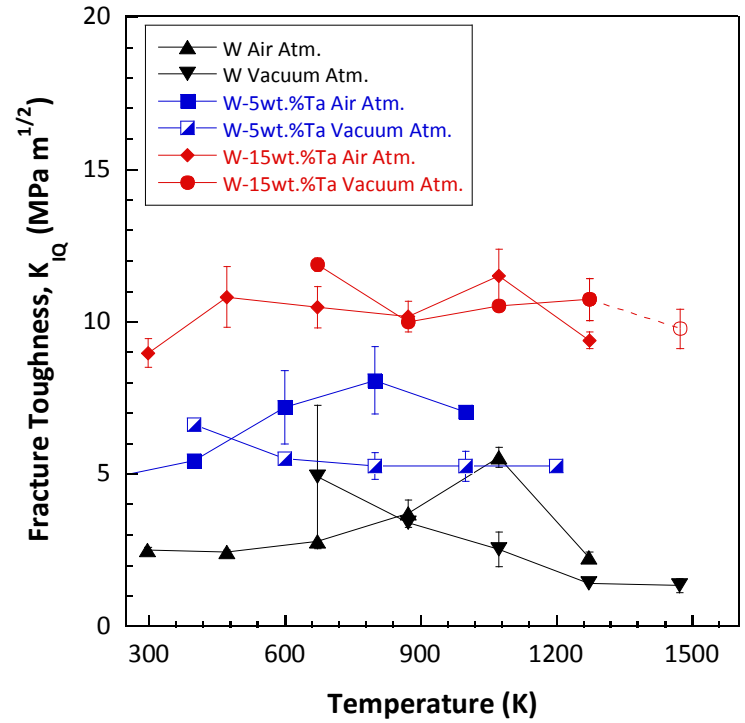

Fig. 10. Nominal fracture toughness of W-5wt. %Ta, W-15wt. %Ta and pure tungsten alloys tested as a function of temperature. The error bars correspond to the standard deviation of the experimental data.

Microstructural heterogeneities in W-5 wt. % Ta, i.e. Ta pools and non-milled W grains, were fractured in a brittle manner with evidence of both intergranular cracking and cleavage (Fig. 10). Due to the fact that our materials retain a sub-granular structure with grains smaller than 100 nm, many small facets can be observed on the fracture surface. Additionally, partially pulled out grains could be regularly found as well as the presence of many small pores mainly on the grain boundaries. These brittle fracture mechanisms were responsible for the low toughness of the materials as shown in Figure 9.

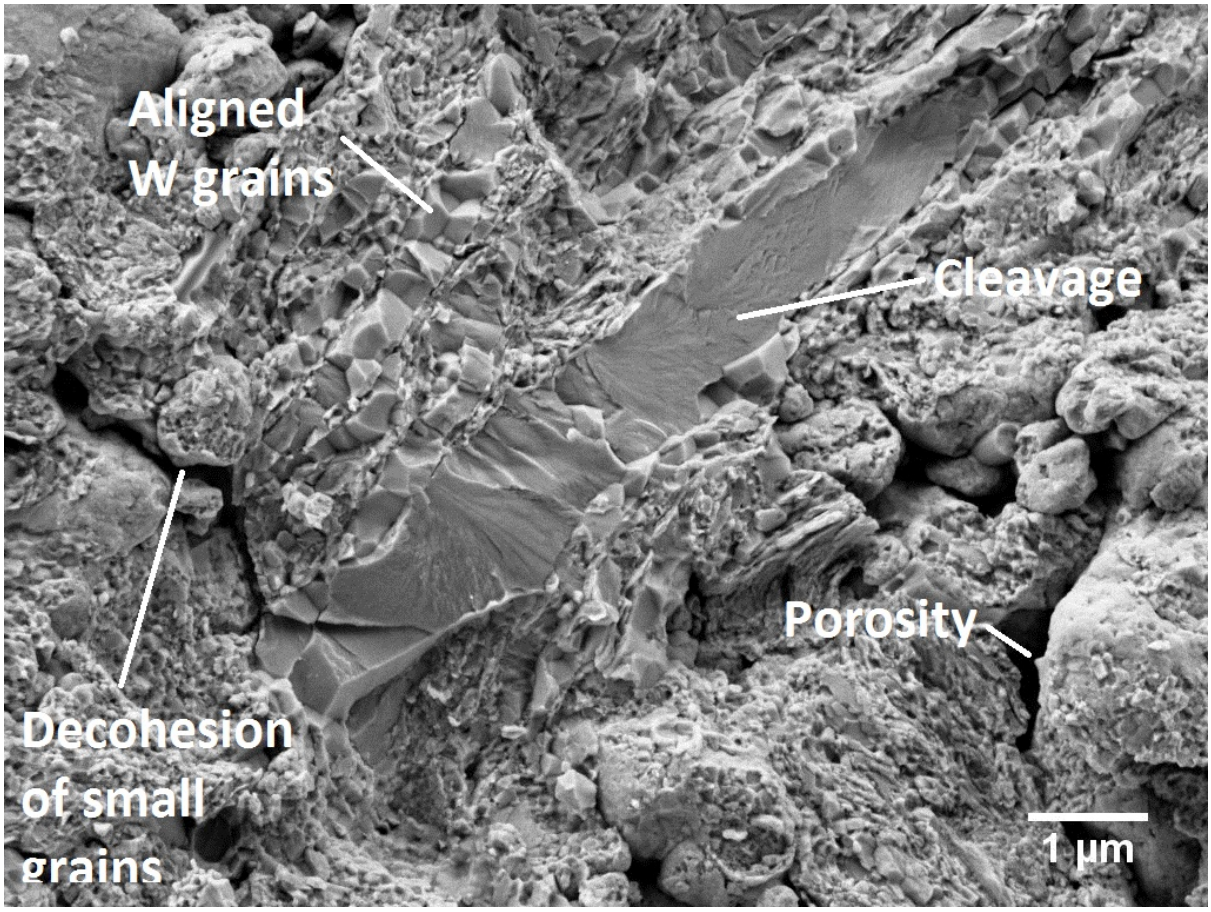

Fig. 11. Fractograph of W-5 wt. % Ta specimen tested at room temperature. As the grains possess subgrains with a size smaller than 1 µm, the micrographs show strongly facetted fracture surfaces, cleavage of coarse grains, aligned W grains and visible porosity.

In contrast to W-5 wt. % Ta, the behaviour of specimens of W-15 wt. % Ta is different: the drop in flexural strength with temperature can be related to the DBTT of this material, taking place at lower temperatures. Whilst at low to moderate temperature, its behaviour is also brittle and shows poor fracture properties. When the temperature increases so does the plastic deformation, showing that the material is fully ductile in the temperature range 1073-1473 K.

The influence on the mechanical properties and on the DBTT of W-5 wt. % Ta has being previously reported with commercial PLANSEE SE forged materials [15]. Those tests also reported an intergranular fracture mode in this system, with the crack propagating from straight through the sample and failing in a brittle intergranular manner.

- ***Fracture Toughness***

Fig. 9 summarises the results of fracture toughness experiments on W-Ta materials over a wide temperature range. As observed in TPB tests, W-5 wt. % Ta specimens failed by brittle fracture at low temperatures.

As K_{IQ} loses validity with increasing ductile behaviour, the calculated values above the transition regime give only a lower bound and are denoted by open symbols. Crack propagates easily through the grain boundaries at low temperatures, reporting low values of fracture toughness.

Those values are in reasonably good agreement with data reported by [16] for tests conducted on W-Ta alloys of nominally 1, 5 and 10 wt. % of tantalum. Even while their investigations were carried out on forged specimens, similar conclusions can be obtained when considering samples with the crack plane parallel to the forging direction. Those authors also reported the increase in fracture toughness with temperature, until a change in fracture behaviour and a drop in global fracture toughness was observed. This maximum value of K_{IQ} that can be observed in Fig. 9 at 1073 K and was explained by [17] as the onset of yielding, i.e. BDTT of the intergranular fracture mode. At higher temperatures, material is ductile so that only blunting of the notch tip occurs. This effect is also more visible in air experiments, where the oxides on the surface of the notch could lead to unreal higher K_{iQ} values.

As opposed to observations after TPB testing, W-15 wt. % Ta specimens show a by far larger amount of trans-crystalline fracture and plastic deformation of grain boundaries compared to W-5 wt. % Ta material (see Fig. 5 and Fig.11). Therefore, the amount of trans-crystalline fracture seems to be correlated to the fracture toughness of the samples as K_{IQ} is about twice as high. For this material, the crack is triggered within the large and linked-up tungsten-tantalum regions as cannot propagate easily within the more brittle phase over long distances.

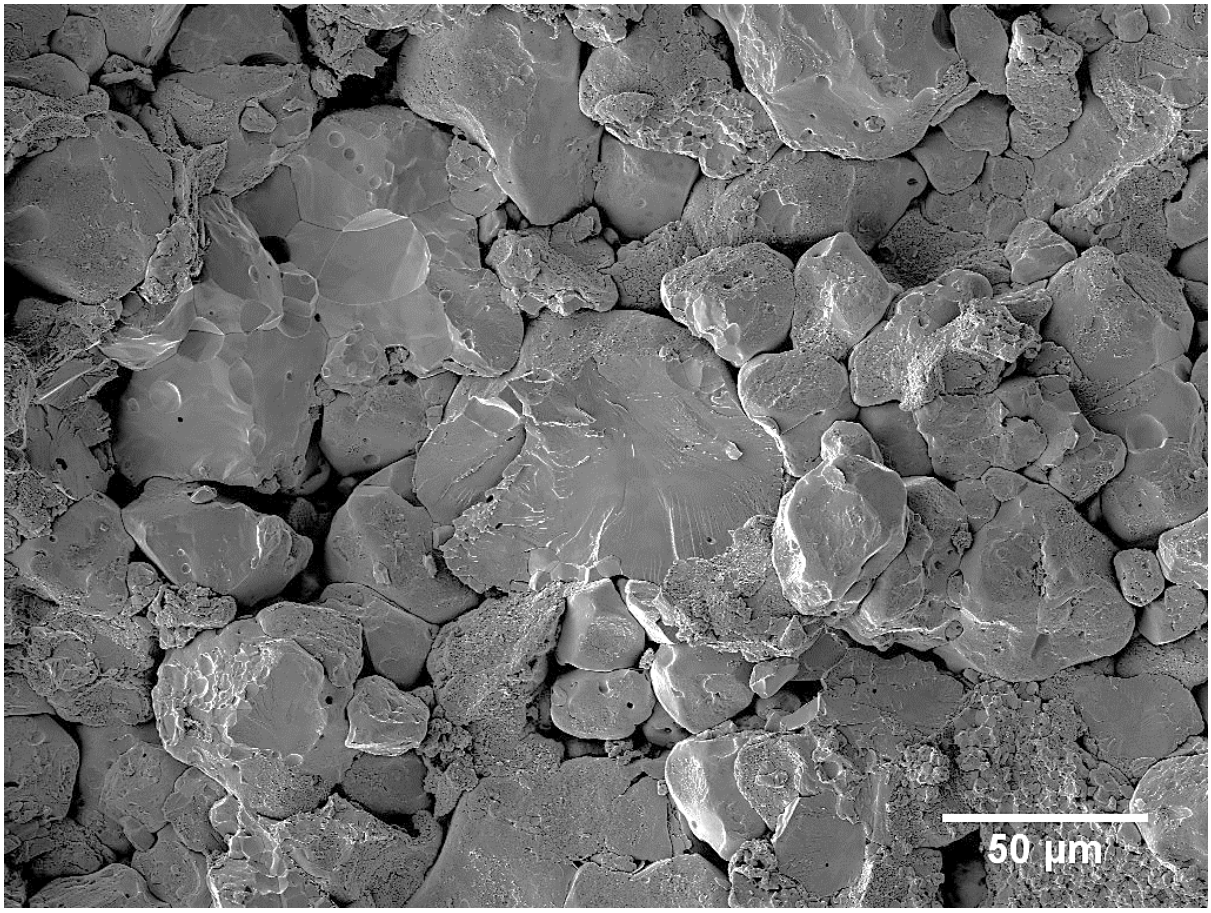

Fig. 12. Fracture surface of W-15 wt. % Ta composite tested at 1473 K in vacuum showing intergranular fracture and cleavage of W grains.

- ***Thermal diffusivity***

The change in thermal diffusivity for the W-Ta materials with temperature is shown in Figure 11. Due to the lack of results for our pure tungsten reference material, those have been compared with two different pure tungsten products: W-UHP, ultra-high-purity tungsten (99.9999 wt. %) [18] and an industrially manufactured tungsten grade [19] processed by the same powdermetallurgy route as our materials. M. Wirtz et al. [18] also tested a commercial W-5 wt. % Ta product, hence their values has also been used as a reference.

Diffusivities of the specimens decreased with an increase of test temperature, though W-Ta systems always have lower values than pure W. The large drop in diffusivity was also observed in pure W; however, this drop seems to be lower for W-15 wt. % Ta hence, the difference with W and W–Ta alloys decreased with increasing temperature.

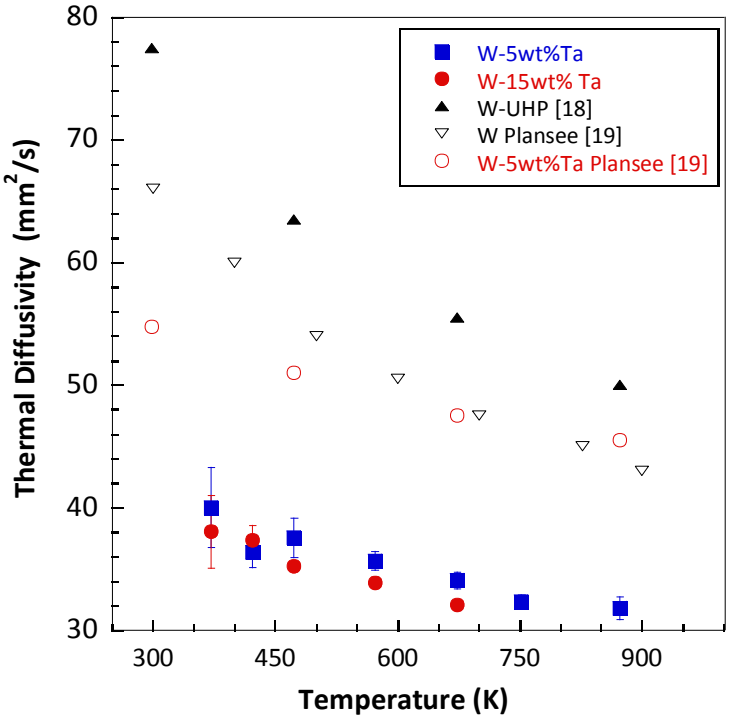

Fig. 13. Thermal Diffusivity of W-15 wt. % Ta, W-5 wt. % Ta [18], W-UHP [18] and pure W [19].

4. Conclusions

Two W-Ta materials were manufactured by hot isostatic pressing using standard powder metallurgy techniques. After HIPing a density around 92 % was achieved for both systems. A very fine microstructure consisting of grains of Ta(W) solid solution, in the submicron range, surrounding Ta pools and non-milled W grains was found in the case of W-5 wt. % Ta. Whereas, W-15 wt. % Ta material presented a biphasic microstructure composed of W and Ta respectively without signs of alloying among the elements.

Their mechanical properties (strength and toughness) were measured by means of three-point bending tests on smooth and notched specimens from 300 K up to 1273 K in air and to 1473K in high vacuum atmosphere. The thermal and mechanical properties of the W-5 wt. % Ta material are dominated by the refined microstructure; it shows a sharp ductile-to brittle transition in the range 1273 to 1323 K, but by contrast, with very poor fracture toughness, due to decohesion of those small grains.

In the case of the W-15 wt. % Ta system, the thermal diffusivity is close to 32 mm^2/s in the maximum temperature tested, 673K, indeed lower than literature references. It exhibits significantly higher fracture toughness and lower DBTT – around 673 K –than the W-5 wt. % Ta material. Therefore, the improvement in toughness of W15Ta system could be attributed to a change in the fracture initiation mechanisms, as the DBTT of this materials is lower.

In any case, the HIP materials are brittle up to very high temperatures, which hamper significantly their workability. A possible way to decrease the DBTT and to increase the strength and fracture elongation of the W-Ta system could be a thermo mechanical treatment at higher temperatures.

Further investigations into the effect of milling time and chemistry are currently on-going, but it appears that tantalum has no beneficial effects on DBTT of tungsten after a milling-HIP processing.

Acknowledgements

This work has been carried out within the framework of the EUROfusion Consortium and has received funding from the Euratom research and training program 2014-2018 under grant agreement No 633053. The views and opinions expressed herein do not necessarily reflect those of the European Commission. In addition, research by E.Tejado was supported by the CSIC (JAE-Predoc program) co-financed by FSE supports. The authors would also like to acknowledge the Ministerio de Economía y Competitividad of Spain for funding for the research project MAT2012-38541-C02-02.

References

[1] Valery Borovikov; Xian-Zhu Tang;Danny Perez; Xian-Ming Bai; Blas P. Uberuaga; Arthur F. Voter. Possible Self-healing in Tungsten under Fusion Reactor Conditions.

[2] Davis, J.W., Slattery, K.T., Barabash, V.R., Makhankov, A., & Ploechl, L. (1998). Assessment of tungsten for use in the ITER plasma facing components. Journal of Nuclear Materials, 258-263(ptA), 308-312.

[3] W.D. Klopp. A REVIEW OF CHROMIUM, MOLYBDENUM, AND TUNGSTEN ALLOYS. Journal of Less-Common Metals, 42 (1975) 261-278.

[4] Mutoh Y., Ichikawa K., Nagata K. and Takeuchi M. 1995. J. Mater. Sci. 30 770–5

[5] Hesch, K.; Aktaa, J.; Antusch, S.; Boccaccini, L.V.; Day, C.; Demange, D.; Fietz, W.; Gantenbein, G.; Möslang, A.; Norajitra, P.; Rieth, M. Technology developments at KIT towards a magnetic confinement fusion power plant. Transactions of Fusion Science and Technology, 61(2012) S.64-69

[6] N. Baluc, et al.Nucl. Fusion, 47 (2007), pp. S696–S717

[7] M.R. Gilbert and J.-Ch. Sublet 2011 Nucl. Fusion 51 043005. Neutron-induced transmutation effects in W and W-alloys in a fusion environment.

[8] Cottrell G.A., Kemp R., Bhadeshia H.K.D.H., Odette G.R. and Yamamoto T. 2007 J. Nucl. Mater. 367-370 603-9

[9] M. Dias, F. Guerreiro, J.B. Guerreiro, A. Galatanu, M. Rosinski, M.A. Monge, E. Alves, P.A Carvalho, “Consolidation of W-Ta composites: hot isostatic pressing and spark and pulse plasma sintering”, submitted in SOFT conference (2014).

[10] T. Palacios et al. Mechanical Characterisation of Tungsten-1 wt.% Yttrium Oxide as a Function of Temperature and Atmosphere. Journal of Nuclear Materials.

[11] W.C. Oliver, G.M. Pharr. An improved technique for determining hardness and elastic modulus using load and displacement sensing indentation experiments. J. Mater. Res, 7 (6) (1992)

[12] G.V. Guinea, J.Y. Pastor, J. Planas and M. Elices. Stress Intensity factor, compliance and CMOD for a general three-point-bend beam. International Journal of Fracture 83: 103-116, 1998.

[13] B.N. Enweani, J.W. Davis, A.A. Haasz. Thermal diffusivity/conductivity of doped graphites. Journal of Nuclear Materials 224 (1995) 245-253

[14] E.O. Hall. Nature, 173 (1954), p. 948

[15] M. Rieth, S.L *et al.,* Recent progress in research on tungsten materials for nuclear fusion applications in Europe, Journal of Nuclear Materials, Volume 432, Issues 1–3, January 2013, Pages 482-500, ISSN 0022-3115

[16] Stefan Wurster, Bernd Gludovatz, Andreas Hoffmann, Reinhard Pippan, Fracture behaviour of tungsten–vanadium and tungsten–tantalum alloys and composites, Journal of Nuclear Materials, Volume 413, Issue 3, 30 June 2011, Pages 166-176.

[17] D.Rupp, S.M. Weygand. Anisotropic fracture behaviour and brittle-to-ductile transition of polycrystalline tungsten. Philosophical Magazine. Vol. 90, Iss. 30, 2010.

[18] M Wirtz et al. Comparison of the thermal shock performance of different tungsten grades and the influence of microstructure on the damage behaviour. 2011 Phys. Scr. 2011-014058

[19] Y.S. Touloukian, R.W. Powell, C.Y. Ho, M.C. Nicolaou, Thermophysical Properties of Matter, Vol. 10: Thermal Diffusivity, IFI/Plenum, New York, 1973.